THE JOURNAL OF PHYSICAL CHEMISTRY C

Article

pubs.acs.org/JPCC

Photophysical Characterization and α-Type Delayed Luminescence of Rapidly Prepared Au Clusters

Buddha Mali, Anatoliy I. Dragan, Jan Karolin, and Chris D. Geddes*

Institute of Fluorescence and Department of Chemistry and Biochemistry, University of Maryland Baltimore County, 701 East Pratt Street, Baltimore, Maryland 21202, United States

ABSTRACT: A new and perspective addition to traditional fluorescent probes is the Au clusters (8−25 atoms) which can label proteins, rendering them extremely bright and photostable. In this paper, we show that albumins can quickly and effectively be labeled using microwave acceleration, which shortens the time of Au labeling from several hours to <30 s. Chromatography of Au proteins and FLIM (fluorescence lifetime imaging microscopy) reveals that Au clusters readily form and remain associated with the proteins. Subsequently, luminescence of the Au proteins (BSA, biotinylated-BSA, HSA) was studied using 3D-emission spectroscopy, time-resolved spectroscopy, and FLIM. We show that the red luminescence of the 25-atom gold cluster attached to the proteins has a broad range of emission lifetimes: about 95% of the total emission has a lifetime component ranging from 0.4 to 105 ns, and ∼5% is a delayed (alpha) emission with a range of lifetimes from 1 to 280 μs. The spectrum of Au delayed emission coincides with its fluorescence spectrum, suggesting that the Au delayed emission is actually delayed fluorescence (possibly, classical α-type), and emitting from the same electronic state. Our findings for the Au proteins suggest their broad applicability as new long-lived luminescence probes for the life sciences.

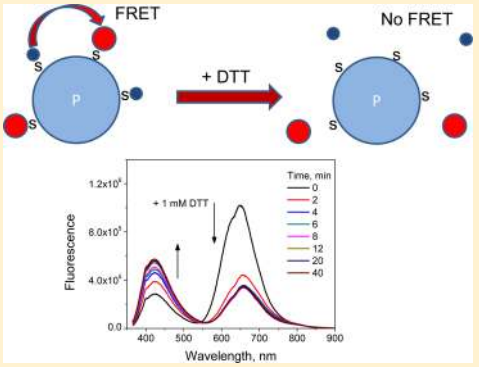

1.0. INTRODUCTION

Fluorescence spectroscopy is a powerful tool in the study of biological macromolecules, their structure, and respective interactions. Due to both a high sensitivity and dynamic range, fluorescence techniques are entrenched throughout the life sciences. Information collected by fluorescence spectroscopy is based on luminophores (intrinsic and extrinsic, fluorescent and phosphorescent), their sensitivity to micro- and macro-environments, their photostability, and the ability to be attached/bound to a certain target and report on probe specific locations.[1]

Labeling of biomolecules (proteins, nucleic acids, etc.) with chromophores is a widely employed approach in numerous biological studies particularly in biomedical assays.[1] A new addition to traditional fluorescent probes is the tiny gold and silver clusters of nanometer and sub-nanometer size. Metal non-plasmonic nanoclusters (NCs) of <2 nm size show photoluminescent properties, which have been used in many biomedical applications, including imaging,[2,3] sensing,[4,5] and macromolecular labeling.[6,7] While plasmonic nanoparticles of sizes >5 nm, characterized by the presence of a plasmon resonance absorption band, are not themselves fluorescent,[8] the fluorescence of the small NCs demonstrates chromophore-like properties, showing discrete electronic-like states and size dependent absorption and emission spectra.[6,8,9] Upon synthesis, the size of a metal NC forms with a specific number of atoms, 8, 11, 13, 18, 22, 25, etc., depending on experimental conditions and the presence of specific templates such as polymers, nucleic acids, or peptides.[2,6,10,11] Accordingly, depending on a NC size, the spectral distribution of NC emission varies from blue (8-atom NC) to red (25-atom NC) and even further into the infrared for larger NCs.[2,6,11] It has been suggested that Au clusters possess two discrete excited states, depending on the spin multiplicity (singlet or triplet), which determines the NC reactivity.[11] Due to an effective oxygen-dependent depopulation of the triplet state, the phosphorescence yield of Au NC is low in solution.[11] Typically, synthesized NCs have a low fluorescence quantum yield, around 10^{-5}−10^{-3}, and subsequently can serve as quenchers for a neighboring fluorophore, utilizing a specific energy transfer mechanism termed nanosurface energy transfer (NSET).[12−14] Also, the relatively low quantum yield of Au clusters synthesized by some methods typically limits their applications in biomedical imaging and their ability to compete with traditional molecular fluorophores.

Recently, it has been shown that metal NCs can grow within proteins (BSA, lysozyme, apoferritin, pepsin)[3,10,15,16] using the proteins as a matrix, which is able to stabilize NCs of specific sizes, namely, 8- and 25-atom NCs, with unique fluorescent properties. Interestingly, Au clusters integrated within proteins readily show very bright fluorescence. These bright Au labeled proteins could potentially be employed in many biomedical applications and assays, where traditional fluorophores are used today. However, the photophysics of these NCs remains complex and ill understood. In this paper, we subsequently study the photophysical behavior of the Au NCs attached to

Received: March 6, 2013
Revised: July 3, 2013
Published: August 1, 2013

   dx.doi.org/10.1021/jp4023184 | J. Phys. Chem. C 2013, 117, 16650−16657

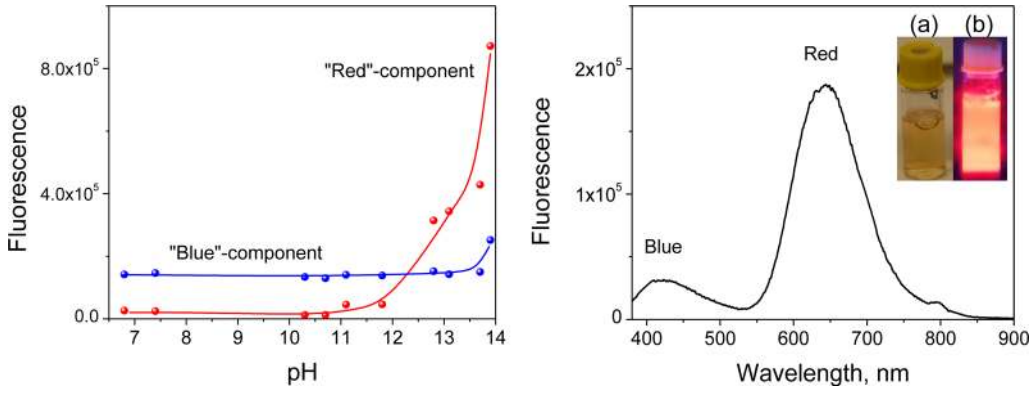

Figure 1. (left) The emission characteristics of Au clusters in the presence of HSA are pH-dependent. Red fluorescence (maximum at 630−650 nm) (~25-atom Au clusters) dramatically increases at high pH > 12. Blue fluorescence (maximum at 430−470 nm), which corresponds to 8-atom Au clusters, forms at neutral pH and does not sufficiently change with pH. Excitation of Au−HSA fluorescence was at 350 nm. (right) Fluorescence spectra of the Au−albumin sample. Excitation was at 350 nm. (Inset) Real-color images of the Au−albumin solution under daylight (a) and UV exposure (b).

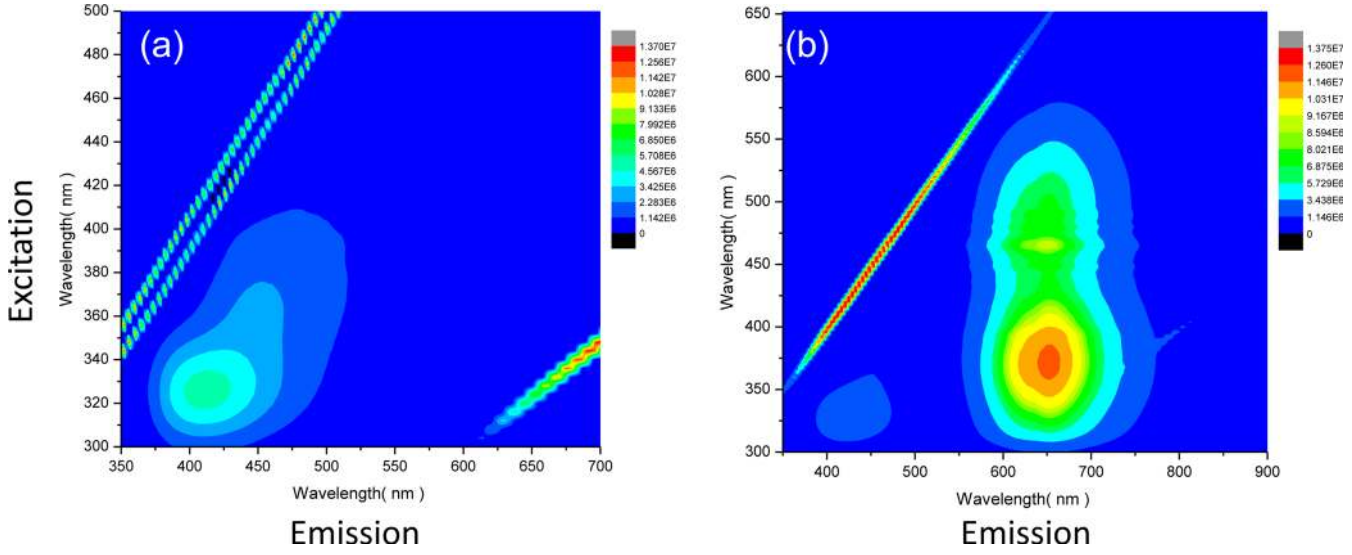

Figure 2. The 3D emission spectra of Au−BSA: (a) blue fluorescent gold, prepared at pH 11; (b) red fluorescent gold, pH 13.9.

proteins (bovine serum albumin and human serum albumin) using several biophysical methods, including time-resolved fluorescence spectroscopy, the FLIM technique, fluorescence anisotropy, and fluorescence 3D spectral analysis. We have also significantly improved the process of Au NC synthesis by employing microwave acceleration.

2.0. MATERIALS AND METHODS

Human serum albumin (HSA) and bovine serum albumin (BSA) were purchased from Sigma-Aldrich. A BSA derivative, biotinylated BSA, was purchased from Fisher. Ascorbic acid and chloroauric acid ($HAuCl_4$) were purchased from Sigma (USA) and have been used as received. Ultrapure water (18 MΩ) was used in all experiments.

Measurements of fluorescence, 3D fluorescence, and emission/excitation spectra, fluorescence anisotropy, and delayed emission decay of the Au protein samples were undertaken using a FluoroMax-4 spectrofluorometer (Horiba, USA), equipped with automated polarizers.

Luminescence decay and excited state lifetimes of the Au clusters/protein samples were both measured and deconvoluted using a Time-Domain TemPro Fluorescence Lifetime System, Horiba Jobin Yvon Inc., USA, and the IBH DAS 6.0 software, respectively.

Analysis of Au fluorescence lifetime distributions in dried Au protein samples was undertaken using fluorescence-lifetime imaging microscopy (FLIM), using an Olympus BX51 confocal microscope, Horiba Jobin Yvon Inc., USA. Samples for FLIM measurements were prepared by drying concentrated solutions of Au proteins at 37 °C until dry.

Au cluster labeling of proteins was undertaken in accordance with ref 2 by adding an aqueous solution of chloroauric acid to protein solutions in water, followed by dropwise addition of the reducing agent (ascorbic acid) to trigger the formation of Au clusters on/within the protein surface. The pH of the reaction was changed by adding NaOH to maintain a pH in the range 8−13. The incubation time was typically 5−6 h at 37 °C. In our new modified protocol, we have used microwave irradiation of the reactive solution for <30 s in a microwave cavity (GE Compact Microwave Model: JES735BF, frequency 2.45 GHz, power 700 W). The microwave power was reduced to 20%, which corresponded to about 140 W over the entire cavity. This now microwave accelerated synthesis reduced the reaction

dx.doi.org/10.1021/jp4023184 | J. Phys. Chem. C 2013, 117, 16650−16657

time from 5−6 h to less than 30 s to produce the otherwise identical product.

3.0. RESULTS AND DISCUSSION

3.1. Au Clusters Formed with HSA at Both an Elevated (37 °C) Temperature and Microwave Acceleration. Formation of the Au clusters in the presence of HSA (10 mg/mL) was undertaken at different pH's using the previously published protocol.[2] The total reaction time for the Au cluster formation was around 6 h.[3,15] Emission of the Au protein samples prepared via *this method* is distributed mostly into two fluorescence spectra (excitation at 350 nm): blue, fluorescence maximum at 430 nm; red, maximum at 650 nm. The observed fluorescence can readily be attributed to the fluorescence of 8- and 25-atom Au clusters.[2,15] The ratio of fluorescence intensities of both the large and small NCs is pH-dependent and increases with the pH of the reaction solution. The red fluorescence becomes dominant at pH > 12. Microwave irradiation of the reaction solution (10 s three times irradiation at 20% power) accelerates the process of Au NC formation. The left side of Figure 1 shows the emission peak intensities for the red and blue components recorded at different pH values. On the right side is the fluorescence spectrum shown for an Au−HSA sample prepared at pH 13.9 and after microwave heating. Under UV light illumination, the solution is highly luminescent (Figure 1, inset). It should be noted that in the microwave synthesis approach the Au NC conjugation to protein is accelerated >1000-fold, offering a rapid approach to synthesis of the Au−protein complexes, producing the same product as the 6 h synthesis.

3.2. Au Clusters Formed with BSA. We have found that Au clusters, conjugated to BSA at different pH's, demonstrate the very similar properties as the Au−HSA samples, i.e., a similar distribution in the Au NC sizes and fluorescence properties (Figures 2 and 3). The lifetime parameters of both Au−BSA and Au−HSA fluorescence are shown in Table 1 and 2. At pH 11, the main component of NCs is small, 8-atom gold NCs that emit blue light at 430 nm. The maximum of the fluorescence excitation spectrum is centered at 325 nm. The Stokes shift is about 100 nm. At elevated pH, 13.9, the main component of Au−HSA fluorescence is a red spectrum with a maximum at 650 nm, which reflects the dominance of larger size NCs. A small contribution of blue fluorescent NCs to the emission spectra is also observed. It should be noted that according to the 3D spectrum (Figures 2 and 3) only two NC fluorescence components are observed: blue (8-atom clusters) and red (25-atom clusters). Subsequently, NCs of intermediate sizes appear not to be made in albumins, consistent with other reports of the non-microwaved prepared samples.[4,7] The fluorescence excitation spectrum of the Au(25) NC has two maxima at about 470 and 370 nm. The Stokes shift for Au(25) is ≈180 nm, which is significantly larger as compared to the blue fluorescent 8-atom NC. Both NCs, Au(8) and Au(25), have discrete emission and excitation bands, and are thought to be related to a HOMO−LUMO (highest occupied molecular orbital−lowest unoccupied molecular orbital) gap, which is relatively large.[8,11]

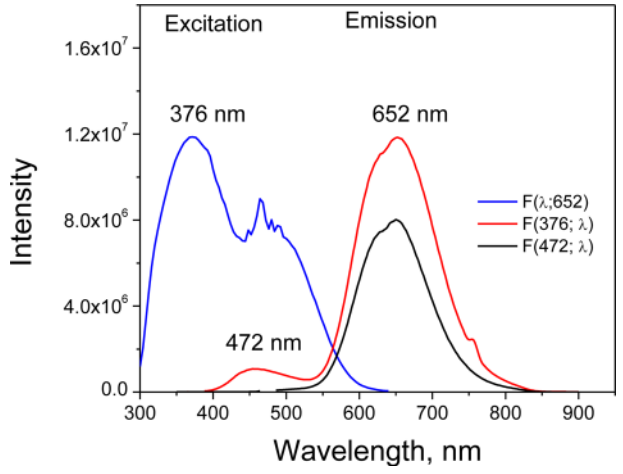

Figure 3. Fluorescence emission and excitation spectra recorded for a typical Au−BSA sample. The fluorescence intensity is in arb. units.

3.3. FLIM Analysis of the Au Clusters. The Au clusters are thought to be strongly conjugated to the host proteins, for both BSA and HSA. FLIM images of the dried protein clusters show the distribution of red fluorescence which is associated with the protein clusters, Figure 4. To analyze excited state lifetimes of the Au−HSA, sample fluorescence decay profiles were collected from 600 points in the area shown in Figure 4, center. Decay curves were fitted to the equation $I(t) = b_1 \exp(-t/\tau_1) + b_2 \exp(-t/\tau_2)$. The statistical distributions of lifetimes and their amplitudes are shown in Figure 4. Normal distribution functions are centered with the following fitting parameters: $\tau_1 = 0.38 \pm 0.12$ ns, $b_1 = 0.79 \pm 0.07$; $\tau_2 = 2.47 \pm 0.70$ ns, $b_2 = 0.21 \pm 0.05$. The fluorescence decay parameters measured by FLIM are in accordance with the parameters measured for the Au(25) protein in solution, cf. Table 1 and Figure 5, except for a long-lived component of $\tau_3 = 27.8$ ns. It is possible that, in a dry sample exposed to air, this component is sufficiently diminished.

3.4. Au Clusters Are Sensitive to Their Environment. A remarkable feature of the Au NCs is that the fluorescence decay parameters are sensitive to the structure of protein and solvent, Figure 5 and Table 1. At a high concentration of GdmCl (8 M), the average lifetime of NCs decreases almost twice as compared to that in PBS buffer, i.e., from 14.2 ns (PBS buffer) to 8.5 ns (8 M GdmCl). This change in lifetime can be explained by protein unfolding in 8 M GdmCl[17,18] and exposure of the gold NCs to the solvent. It is notable that the change in amplitude weighted lifetime is mostly due to a decrease in its long-lived component (Table 1). It changes from 27.8 ns (PBS) to 20.8 ns (GdmCl). The longer-lived excited state of the Au(25) cluster is more sensitive to the microenvironment than the short-lived

Table 1. Parameters of Au−BSA Fluorescence Decay in Different Solutions

Au−BSA	b_1	τ_1 (ns)	b_2	τ_2 (ns)	b_3	τ_3 (ns)	$\langle\tau\rangle^a$ (ns)	χ^2
PBS	37.8	2.95	15.3	0.41	46.9	27.8	14.2	1.32
8 M GdmCl	46.6	2.81	19.3	0.41	34	20.8	8.5	1.44
98% glycerol	57.7	3.1	10.97	0.62	31.3	9.7	4.9	1.16

[a] $\langle\tau\rangle$: amplitude weighted lifetime.

dx.doi.org/10.1021/jp4023184 | J. Phys. Chem. C 2013, 117, 16650−16657

Table 2. Parameters of Au−HSA Fluorescence Decay in PBS

sample	b_1	τ_1 (ns)	b_2	τ_2 (ns)	b_3	τ_3 (ns)	$\langle\tau\rangle^a$ (ns)	χ^2
Au−HSA	9.77	0.57	20.4	4.27	69.84	148	104.29	1.38

[a] $\langle\tau\rangle$: amplitude weighted lifetime.

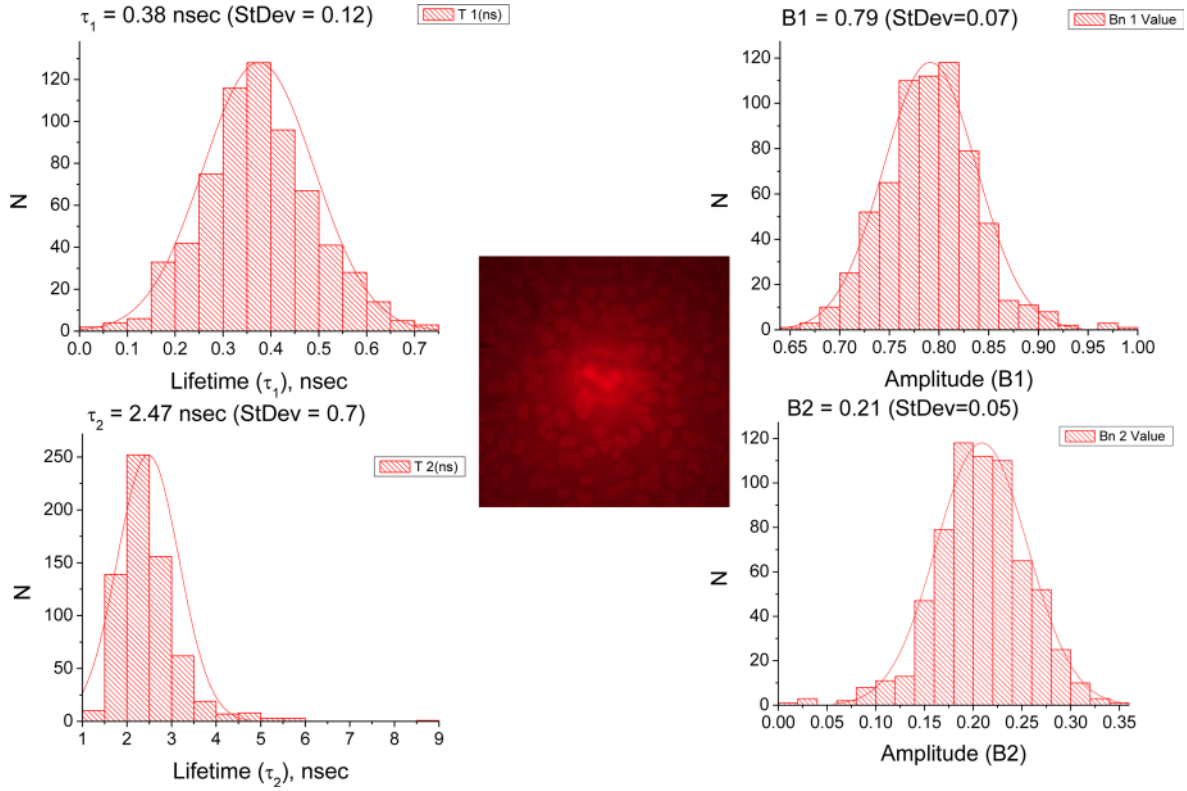

Figure 4. Statistical analysis of lifetimes and amplitudes of Au−HSA fluorescence decays measured by FLIM. Solid lines show the normal distribution of the parameters. The total number of points (decay curves) is 660. Inset (center): Confocal fluorescence image of Au−HSA.

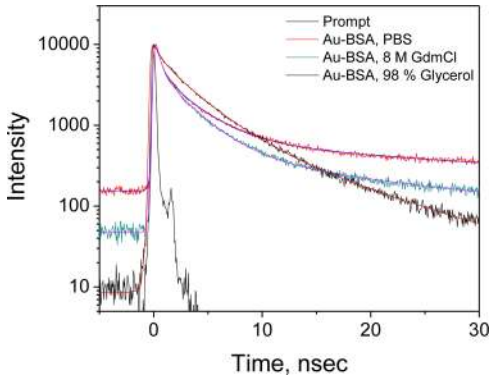

Figure 5. Time resolved fluorescence decays of Au−BSA in PBS, 8 M GdmCl, and 98% glycerol. Excitation of emission was undertaken at 444 nm using a pulsed laser diode.

components, which likely reflects diffusion controlled quenching by dissolved O_2.

The long-lived component of the decay is also sensitive to solvent properties, in particular to the viscosity. In 98% glycerol, the long lifetime (τ_3) of Au(25) decreases 3-fold, from 14.2 ns (PBS) to 4.9 ns (glycerol), while shorter lifetimes (τ_1 and τ_2) are almost constant (Table 1). This observation also suggests an O_2 quenching mechanism.

3.5. Au Cluster Long-Lived Luminescence. The change in the long-lived component of the decay correlates well with the change in magnitude of a background-like signal observed at times before the prompt, i.e., at $t < 0$, Figure 5, in the time-resolved decays. The origin of this signal can be explained by the contribution of a delayed long-lived emission, which results in a background-like signal registered in the nanosecond time window. The "background" signal for the Au−HSA sample in PBS is ∼200 counts, which is ∼5% of the maximum 10 000 counts, Figure 6.

For further characterization of the delayed emission of the Au NCs, we have measured the emission decay functions over a broad range of times, from microseconds to milliseconds, Figure 7a,b and Table 3. The decay function shown in Figure 7b was registered using an initial delay time of 50 μs to measure the longer-lived excited states of NCs (Table 3). Analysis of the data shows a broad distribution of delayed emission lifetimes, ranging from 0.05 to 280 μs, Tables 3 and 4.

A remarkable feature of the delayed emission is that its spectrum directly coincides with the steady-state fluorescence spectrum of the Au NCs. This suggests that the observed delayed emission (luminescence) occurs from the same excited singlet state as the short-lived fluorescence, simply delayed in time. To the best of our knowledge, this is the first observation of delayed (long-lived) fluorescence from Au clusters in solution for microwave synthesized and the 6 h synthesis Au

dx.doi.org/10.1021/jp4023184 | J. Phys. Chem. C 2013, 117, 16650−16657

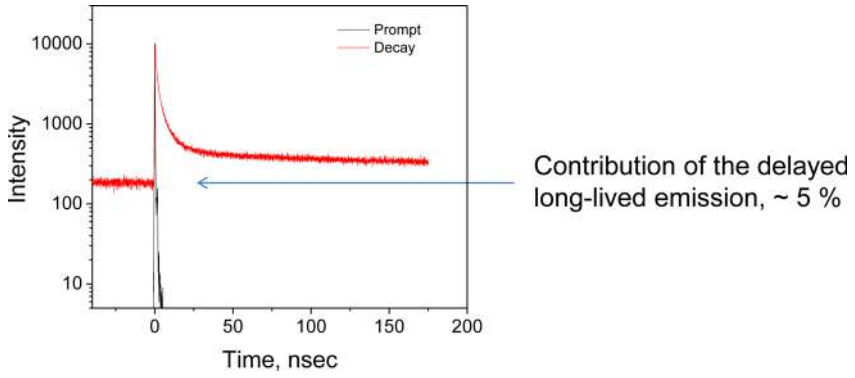

Figure 6. Time resolved fluorescence decays of Au−HSA in PBS.

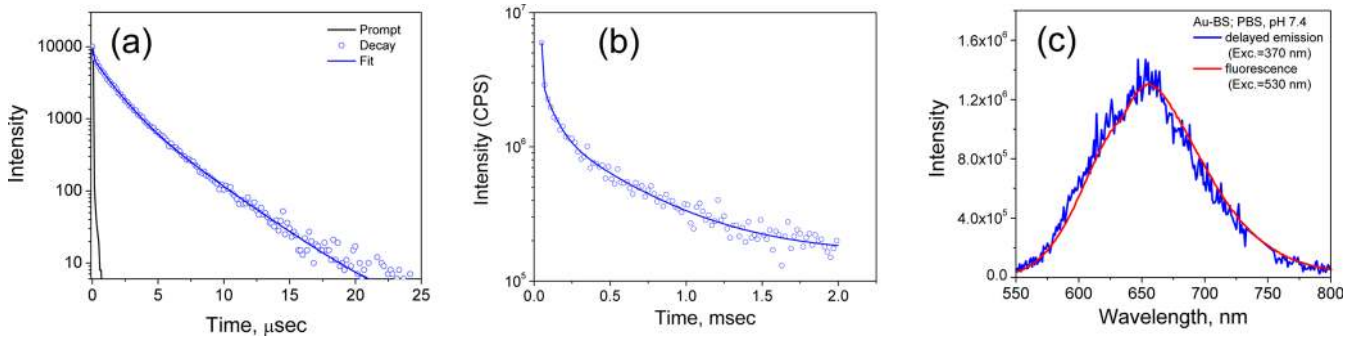

Figure 7. (a, b) Profiles of Au−HSA emission decay measured in the time-domain. (c) Fluorescence spectra of Au clusters and their delayed emission spectra coincide; i.e., delayed emission is not "phosphorescence". The shape and position of the fluorescence spectrum and delayed emission do not depend on excitation wavelength in the range (300−530 nm).

Table 3. Parameters of Au−HSA Delayed Emission Decay in PBS

sample	b_1	τ_1 (μs)	b_2	τ_2 (μs)	b_3	τ_3 (μs)	$\langle\tau\rangle^a$ (μs)	χ^2	time-domain instrument
Au−HSA	50.4	0.05	34.04	1.39	15.54	3.43	1.03	1.12	TemPro
Au−HSA	39.8	4.3	31.2	28.3	29.0	281.0	92.1		FluoroMax

$^a\langle\tau\rangle$: amplitude weighted lifetime.

Table 4. Parameters of Au−BSA Delayed Emission Decay in Different Solutions (Ex. = 493 nm)

Au−BSA	b_1	τ_1 (μs)	b_2	τ_2 (μs)	b_3	τ_3 (μs)	$\langle\tau\rangle^a$ (μs)	χ^2
PBS	49.65	1.4	14.4	0.19	35.94	2.94	1.78	1.2
8 M GdmCl	39.8	1	36.47	0.052	24.34	2.2	0.95	1.14
98% glycerol	55.6	1.9	3.04	0.39	41.35	4.24	2.8	1.16

$^a\langle\tau\rangle$: amplitude weighted lifetime.

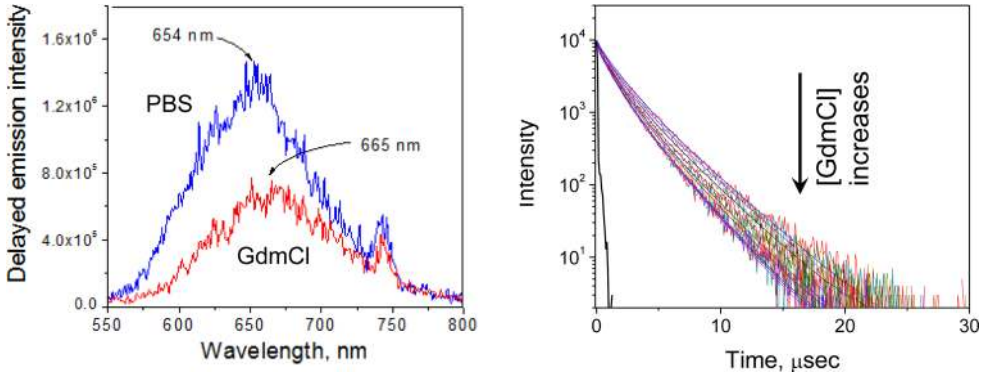

Figure 8. (left) Delayed emission spectra of Au−BSA in PBS and in 8 M GdmCl at ambient temperature. (right) Delayed emission profiles of Au−BSA at different concentrations of denaturant, GdmCl.

dx.doi.org/10.1021/jp4023184 | J. Phys. Chem. C 2013, 117, 16650−16657

clusters. The mechanism of this phenomenon is unknown at present, but we suggest at least two possible explanations for the NC delayed emission. One is that the electronic system of Au clusters has two different excited states depending on the spin multiplicity (singlet (S1) or triplet (T))[11] and the transition to a singlet state, $T \rightarrow S_1$, is more probable than radiational depopulation of the triplet state, $T \rightarrow S_0$, i.e., phosphorescence. Another possible mechanism of the delayed luminescence is an excited electron trapping, followed by release to the S_1 state. Au clusters grow in protein cavities and, subsequently, are in tight contact with different protein groups, which potentially could trap excited electrons within the protein matrix. Assuming that the environment of NCs in protein cavities is heterogeneous, and the fact that we observe a broad distribution of lifetimes, the second mechanism is likely to be more plausible.

3.6. Effect of the Environment on Long-Lived Luminescence. The influence of protein structure on the *delayed emission* was studied by protein unfolding in solutions with the different concentrations of GdmCl. Figure 8 shows the change in the delayed emission spectra of Au NCs and the respective emission decay functions upon BSA unfolding by GdmCl. The delayed emission spectrum shifts to the red by ~10 nm, and its intensity decreases ~2-fold. The red-shift in spectra suggests an increasing solvent/environment polarity, which certainly occurs upon protein denaturation and exposure of the Au clusters to water. Interestingly, the changes in emission spectra are accompanied with a decrease in the Au NC lifetime, Figure 9 and Table 5. The dependence of the Au NC lifetime upon the concentration of GdmCl is thought to correspond to BSA unfolding. The observed changes in emission spectra intensity and NC lifetime can be explained, in particular, by an increase in the rate of Au NC delayed emission quenching by oxygen, which is a well-known effective quencher of triplet states.[19]

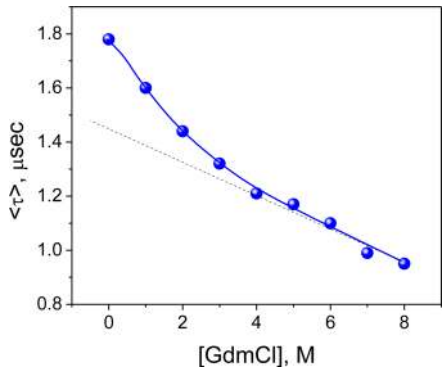

Figure 9. Dependence of the amplitude wieghted lifetime of delayed emission of Au–BSA upon concentration of GdmCl in solution. The dashed line is a linear fitting of the lifetime data measured at GdmCl > 4 M, i.e., at a concentration when BSA is fully unfolded.

Au NCs are known to grow within/on the protein surface to different sizes. As it was shown above, there are mostly two classes of NC sizes (8 and 25 atoms) that show two distinct absorption and fluorescence spectra (Figures 2 and 3). The origin of Au NC attachment to albumin proteins (BSA, HSA) is unknown today, but one can speculate that the sulfhydryl groups of the protein (cysteine residues) may play a role in anchoring gold particles, given the affinity of gold for SH groups. To check this suggestion, we have used the well-known redox reagent, dithiothreitol (DTT), which can effectively disrupt metal–SH bonds. Figure 10 shows the influence of DTT (1 mM) on fluorescence spectra of Au NCs (using an excitation wavelength of 350 nm, one can observe fluorescence of both Au clusters, i.e., blue of Au(8) and red of Au(25)). Notably, in the presence of DTT, the blue fluorescence increases but the red fluorescence simultaneously decreases with time of incubation (Figure 10, left). The observed transformations in spectra can be explained by FRET between the Au clusters (Au(8) and Au(25)) conjugated to the same protein molecule. In fact, the fluorescence spectrum of Au(8) overlaps well with the absorption (excitation) spectra of Au(25), Figure 2, making Au(8) and Au(25) clusters suitable energy transfer donor–acceptor pairs. Subsequently, dissociation of the Au NCs from the protein reduces the number of donor–acceptor pairs on the surface and shows characteristic FRET change in their intensities. Figure 10 presents a model explaining the observed changes in the Au protein system upon exposure to DTT.

We also have studied the influence of DTT on the Au–protein conjugation using chromatography (Figure 11). In the presence of DTT, the fluorescence intensity of the purified protein (purified from unbound NCs) shows the same FRET changes in spectra as the solution experiments; some NCs still are bound to protein even after incubation with an elevated concentration of DTT (5 mM). Subsequently, we suggest that Au NCs, both Au(8) and Au(25), are strongly conjugated to protein (albumins), causing FRET between NCs; NCs are stabilized on the protein surface by bonding to sulfhydryl groups (Cys residues) and can be removed by adding DTT to the solution; residual NCs, which could not be removed by DTT, possibly interact with other protein groups, which in turn stabilize the NC/protein complex.

Table 5. Parameters of the Decay of Delayed Emission of Au–BSA in PBS for Different Concentrations of GdmCl

[GdmCl] (M)	b_1	τ_1 (μs)	b_2	τ_2 (μs)	b_3	τ_3 (μs)	$\langle\tau\rangle^a$ (μs)	χ^2
0	49.65	1.4	14.4	0.19	35.94	2.94	1.78	1.2
1	47.59	1.31	18.67	0.095	33.36	2.86	1.6	1.2
2	46.59	1.24	22.21	0.08	31.21	2.72	1.44	1.1
3	45.52	1.237	26.28	0.085	28.21	2.62	1.32	1.15
4	44.73	1.18	27.83	0.081	27.4	2.48	1.21	1.06
5	44.58	1.125	28.57	0.075	26.86	2.4	1.17	1.06
6	44.81	1.1	29.48	0.086	25.71	2.28	1.1	0.98
7	40.98	1.05	35.34	0.063	23.68	2.27	0.99	1.17
8	39.18	1	36.47	0.052	24.34	2.2	0.95	1.14

[a] $\langle\tau\rangle$: amplitude weighted lifetime.

dx.doi.org/10.1021/jp4023184 | J. Phys. Chem. C 2013, 117, 16650–16657

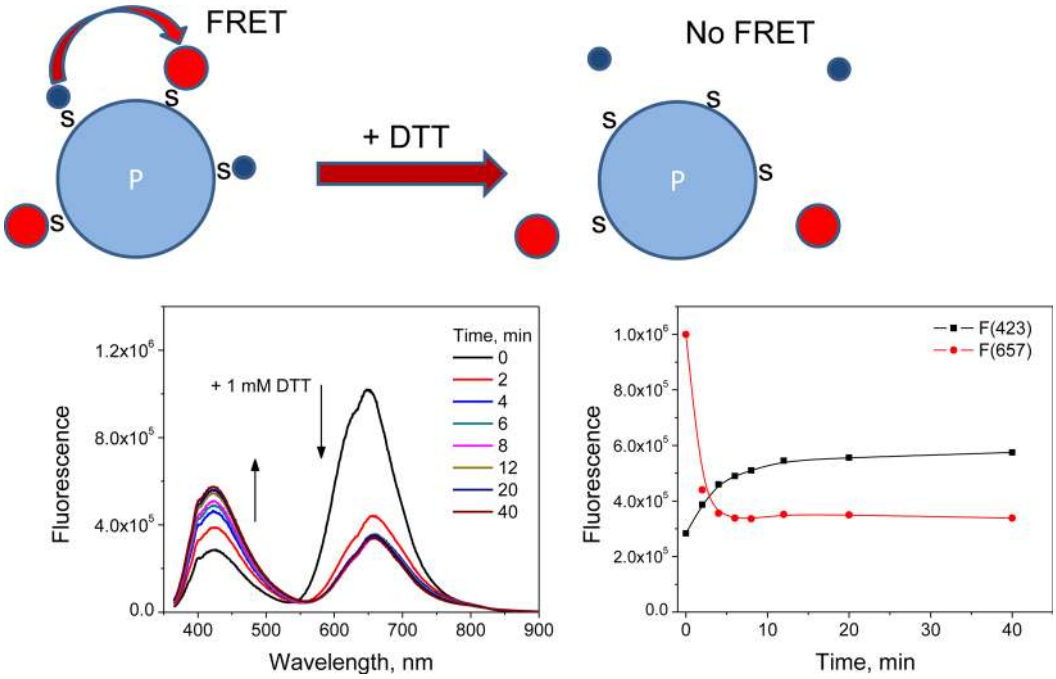

Figure 10. (cartoon) DTT induces dissociation of Au clusters from protein, which decrease interparticle FRET. P, protein; red and blue circles, Au clusters. (bottom, left) Time dependent change in the fluorescence spectrum of the Au–BSA sample in the presence of 1 mM DTT. (bottom, right) The dependence of "blue" and "red" fluorescence intensity upon time after addition of 1 mM GdmCl into solution, PBS, pH 7.4.

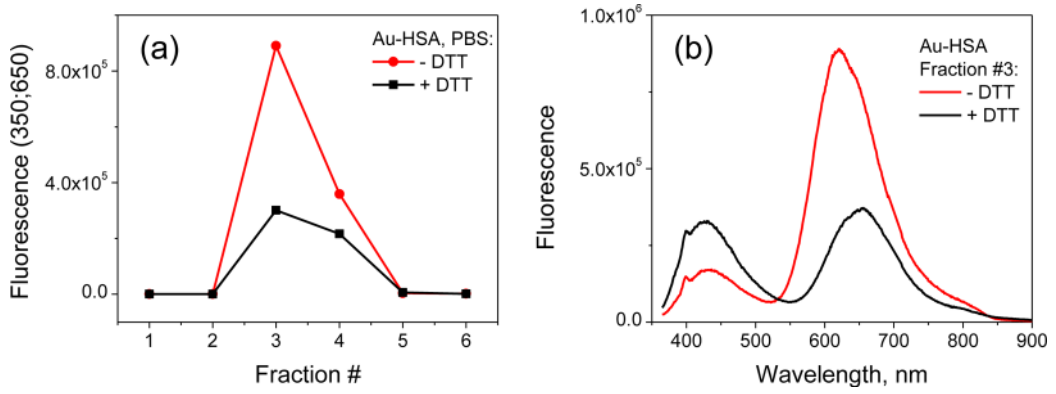

Figure 11. (a) Elution profiles of Au–HSA samples in PBS and PBS + 5 mM DTT. For analysis, Bio-Rad BioGel P-30 Fine Purification resin was used to separate free dye/Au clusters from proteins with MW > 40 000. After-column solutions were collected in 1 mL fractions. For the registration of protein fractions conjugated with gold clusters, each fraction was measured by fluorescence using a FluoroMax fluorometer. Excitation, 350 nm; registration at 650 nm. (b) Fluorescence spectra of fraction #3 of the Au–HSA samples in PBS and PBS + 5 mM DTT.

4.0. CONCLUSIONS

In this paper, we report that rapid microwave acceleration enables both 8- and 25-atom Au–protein complexes to be synthesized. This method of NC preparation produces NCs with identical properties as those for the NCs prepared by the lengthy 6 h synthesis method.

We have found that the NCs display a long-lived *alpha-type luminescence*, which can readily be quenched by either the HSA or BSA denaturing in the presence of GdmCl. We propose that the denaturation of the complex readily allows dissolved oxygen to quench the complex. In addition, studies to release the Au atom clusters from within the proteins which are held by the association with sulfhydryl groups reveal a possible FRET mechanism between the 8-atom (donor) and 25-atom (acceptor) clusters. Interestingly, a subpopulation of clusters is also present, which is unaffected by the presence of DTT, even in the presence of denaturant, suggesting some clusters to be stabilized by other protein groups.

■ AUTHOR INFORMATION

Corresponding Author

*Phone: +1-410-576-5723. Fax: +1-410-576-5722. E-mail: chrisgeddes72@gmail.com.

Notes

The authors declare no competing financial interest.

■ ACKNOWLEDGMENTS

The authors would also like to thank the Institute of Fluorescence and the Department of Chemistry and Biochemistry at the University of Maryland, Baltimore County (UMBC), for salary support. The authors also acknowledge the support of the NIH NIAID 2084 A1087168-10.

REFERENCES

(1) Lakowicz, J. R. *Principles of Fluorescence Spectroscopy*, 3rd ed.; Springer: New York, 2006.

(2) Retnakumari, A.; Setua, S.; Menon, D.; Ravindran, P.; Muhammed, H.; Pradeep, T.; Nair, S.; Koyakutty, M. Molecular-Receptor-Specific, Non-Toxic, near-Infrared-Emitting Au Cluster-Protein Nanoconjugates for Targeted Cancer Imaging. *Nanotechnology* **2010**, *21*, 055103.

(3) Sun, C. J.; Yang, H.; Yuan, Y.; Tian, X.; Wang, L. M.; Guo, Y.; Xu, L.; Lei, J. L.; Gao, N.; Anderson, G. J.; Liang, X. J.; Chen, C. Y.; Zhao, Y. L.; Nie, G. J. Controlling Assembly of Paired Gold Clusters within Apoferritin Nanoreactor for in Vivo Kidney Targeting and Biomedical Imaging. *J. Am. Chem. Soc.* **2011**, *133*, 8617.

(4) Muhammed, M. A. H.; Verma, P. K.; Pal, S. K.; Retnakumari, A.; Koyakutty, M.; Nair, S.; Pradeep, T. Luminescent Quantum Clusters of Gold in Bulk by Albumin-Induced Core Etching of Nanoparticles: Metal Ion Sensing, Metal-Enhanced Luminescence, and Biolabeling. *Chem.—Eur. J.* **2010**, *16*, 10103.

(5) Wei, H.; Wang, Z. D.; Yang, L. M.; Tian, S. L.; Hou, C. J.; Lu, Y. Lysozyme-Stabilized Gold Fluorescent Cluster: Synthesis and Application as Hg2+ Sensor. *Analyst* **2010**, *135*, 1406.

(6) Lin, C. A. J.; Yang, T. Y.; Lee, C. H.; Huang, S. H.; Sperling, R. A.; Zanella, M.; Li, J. K.; Shen, J. L.; Wang, H. H.; Yeh, H. I.; Parak, W. J.; Chang, W. H. Synthesis, Characterization, and Bioconjugation of Fluorescent Gold Nanoclusters toward Biological Labeling Applications. *ACS Nano* **2009**, *3*, 395.

(7) Richards, C. I.; Choi, S.; Hsiang, J. C.; Antoku, Y.; Vosch, T.; Bongiorno, A.; Tzeng, Y. L.; Dickson, R. M. Oligonucleotide-Stabilized Ag Nanocluster Fluorophores. *J. Am. Chem. Soc.* **2008**, *130*, 5038.

(8) Varnavski, O.; Ramakrishna, G.; Kim, J.; Lee, D.; Goodson, T. Critical Size for the Observation of Quantum Confinement in Optically Excited Gold Clusters. *J. Am. Chem. Soc.* **2010**, *132*, 16.

(9) Wu, Z. K.; Jin, R. C. On the Ligand's Role in the Fluorescence of Gold Nanoclusters. *Nano Lett.* **2010**, *10*, 2568.

(10) Kawasaki, H.; Hamaguchi, K.; Osaka, I.; Arakawa, R. pH-Dependent Synthesis of Pepsin-Mediated Gold Nanoclusters with Blue Green and Red Fluorescent Emission. *Adv. Funct. Mater.* **2011**, *21*, 3508.

(11) Sakamoto, M.; Tachikawa, T.; Fujitsuka, M.; Majima, T. Photochemical Reactivity of Gold Clusters: Dependence on Size and Spin Multiplicity. *Langmuir* **2009**, *25*, 13888.

(12) Chowdhury, S.; Wu, Z. K.; Jaquins-Gerstl, A.; Liu, S. P.; Dembska, A.; Armitage, B. A.; Jin, R. C.; Peteanu, L. A. Wavelength Dependence of the Fluorescence Quenching Efficiency of Nearby Dyes by Gold Nanoclusters and Nanoparticles: The Roles of Spectral Overlap and Particle Size. *J. Phys. Chem. C* **2011**, *115*, 20105.

(13) Jennings, T. L.; Singh, M. P.; Strouse, G. F. Fluorescent Lifetime Quenching near d=1.5 nm Gold Nanoparticles: Probing NSET Validity. *J. Am. Chem. Soc.* **2006**, *128*, 5462.

(14) Yun, C. S.; Javier, A.; Jennings, T.; Fisher, M.; Hira, S.; Peterson, S.; Hopkins, B.; Reich, N. O.; Strouse, G. F. Nanometal Surface Energy Transfer in Optical Rulers, Breaking the FRET Barrier. *J. Am. Chem. Soc.* **2005**, *127*, 3115.

(15) Le Guevel, X.; Hotzer, B.; Jung, G.; Hollemeyer, K.; Trouillet, V.; Schneider, M. Formation of Fluorescent Metal (Au, Ag) Nanoclusters Capped in Bovine Serum Albumin Followed by Fluorescence and Spectroscopy. *J. Phys. Chem. C* **2011**, *115*, 10955.

(16) Panzner, M. J.; Bilinovich, S. M.; Youngs, W. J.; Leeper, T. C. Silver Metallation of Hen Egg White Lysozyme: X-ray Crystal Structure and NMR Studies. *Chem. Commun.* **2011**, *47*, 12479.

(17) Kamal, J. K. A.; Zhao, L.; Zewail, A. H. Ultrafast Hydration Dynamics in Protein Unfolding: Human Serum Albumin. *Proc. Natl. Acad. Sci. U.S.A.* **2004**, *101*, 13411.

(18) Wallevik, K. Reversible Denaturation of Human Serum Albumin by pH, Temperature, and Guanidine Hydrochloride Followed by Optical Rotation. *J. Biol. Chem.* **1973**, *248*, 2650.

(19) Lakowicz, J. R.; Weber, G. Quenching of Fluorescence by Oxygen. Probe for Structural Fluctuations in Macromolecules. *Biochemistry* **1973**, *12*, 4161.